Journal of Chemical Health Risks

www.jchr.org

JCHR (2024) 14(4), 1516-1528 | ISSN:2251-6727

In-vitro and In-vivo Characterization of Gold Nanoparticles for the Treating of Inflammatory Bowel Disease

Vinal Adil[1], Neha Sharma[2], Sharang Bali*[3], Pankaj Masih[3], Ritesh Jain[3], Vinay Kumar[4], Vivek Sahu[5], Jhakeshwar Prasad[6]

[1]Rungta College of Pharmaceutical Sciences and Research, Kohka, Kurud – 490024, Bhilai, Chhattisgarh, India

[2]Faculty of Pharmacy, Bharti Vishwavidyalaya, Durg – 491221, Chhattisgarh, India

[3]School of Pharmacy Chouksey Engineering College, Lal Khadan Masturi Road, Bilaspur - 495004, Chhattisgarh, India

[4]Faculty of Pharmaceutical Sciences, Shri Shankaracharya Technical Campus, Junwani – 490020, Bhilai, Chhattisgarh, India

[5]Kamla Institute of Pharmaceutical Sciences - Shri Shankaracharya Professional University, Junwani - 490020, Bhilai, Chhattisgarh, India

[6]Shri Shankaracharya College of Pharmaceutical Sciences, Junwani – 490020, Bhilai, Chhattisgarh, India

*Corresponding Author Email - spharmacognosy81@gmail.com

(**Received**: 14 April 2024 **Revised**: 01 May 2024 **Accepted**: 18 June 2024)

KEYWORDS
Nanozyme; Inflammatory bowel disease; Reactive oxygen species; Ceria nanoparticles; Antioxidant

ABSTRACT:
The excessive reactive oxygen species (ROS) is a hallmark associated with the initiation and progression of inflammatory bowel disease (IBD), which execrably form a vicious cycle of ROS and inflammation to continually promote disease progression. Here, the gold nanoparticles-embedded ceria nanoparticles (Au/CeO2) with enhanced antioxidant activities are designed to block this cycle reaction for treating IBD by scavenging overproduced ROS. The Au/CeO2 with core-shell and porous structure exhibits significantly higher enzymatic catalytic activities compared with commercial ceria nanoparticles, likely due to the effective exposure of catalytic sites, higher content of Ce (III) and oxygen vacancy, and accelerated reduction from Ce (IV) to Ce (III). Being coated with negatively-charged hyaluronic acid, the Au/CeO2HA facilitates accumulation in inflamed colon tissues via oral administration, reduces pro-inflammatory cytokines, and effectively alleviates colon injury in colitis mice. Overall, the Au/CeO2HA with good biocompatibility is a promising nano-therapeutic for treating IBD.

1. Introduction

Inflammatory bowel disease (IBD) is a chronic inflammatory syndrome of intestine, mainly including ulcerative colitis (UC) and Crohn's disease (CD). Such inflammatory diseases are incurable and severely impair patients' quality of life by diarrhea, abdominal pain, bloody stools, and other extraintestinal manifestations [1]. The mainstay treatment agents for IBD include aminosalicylates, corticosteroids, antibiotics, and immunomodulatory agents aiming to alleviate inflammation and maintain remission. However, these medications are limitedly effective and associated with serious side effects [2], resulting in low patient compliance and economic burden. Biological agents (e.g., infliximab, adalimumab, natalizumab) offer an alternative opportunity for patients that show inadequate responses to standard medicine, but they suffer from limited clinical remission rate, long-term safety, and immunogenicity [3]. Therefore, it is highly desirable to develop innovative strategies for IBD treatment. Despite the etiology of IBD remains unclear, extensive evidence reveals that elevated reactive oxygen species (ROS) is a hallmark in the initiation and during progression of IBD, which correlates with clinical features and IBD-associated colorectal cancer [4]. During the inflammatory episodes, the intestinal mucosa is infiltrated with inflammatory cells and these activated immune cells continuously produce and release free radicals resulting in oxidative stress. The excessive ROS crushes innate antioxidant systems and oxidizes biomolecules (proteins, lipids, and nucleic acids) [5] to cause intestinal epithelium damage. The chain reactions further increase the infiltration of inflammatory cells and promote the production of ROS and inflammatory

Journal of Chemical Health Risks

www.jchr.org

JCHR (2024) 14(4), 1516-1528 | ISSN:2251-6727

cytokines. The vicious cycle of ROS and inflammation continually advances the progression of IBD [6]. Hence, re-establishing redox homeostasis to block this cycle reaction would be a promising strategy for treating IBD. Exogenous natural antioxidant enzymes have been used to neutralize ROS or suppress inflammation for IBD treatment which however are limited by low stability, high cost, and potential immunogenicity. With the development of nanotechnology, nanomaterials with enzymatic catalytic activities have attracted extensive attention as potential candidates for modulating redox homeostasis in IBD [7]. As a representative nanozyme, ceria nanoparticles have been found to possess unique superoxide dismutase (SOD) and catalase (CAT)-mimic activities, which are widely harnessed in the treatment of ROS-related diseases such as androgenetic alopecia hepatic injury kidney injury. Alzheimer's disease and stroke and demonstrated to be biocompatible *in vitro* and *in vivo* [8]. The SOD- and CAT-mimetic activities of ceria originate from the co-existence of cerium (III) and cerium (IV) on the surface. The cerium (III) mainly takes advantage of SOD-mimetic activity to remove O2 •- associated with oxidization of cerium (III) to cerium (IV), whereas the cerium (IV) decomposes H2O2 to mimic CAT associated with reduction of cerium (IV) [9]. Thus, ceria's catalytic activities are highly dependent on the regenerative redox switching between cerium (III) and cerium (IV). However, the reduction rate from cerium (IV) to cerium (III) is impeded because this process is energetically unfavorable. Accelerating the regeneration from cerium (IV) to cerium (III) by facilitating electron transfer might be a feasible strategy to optimize the enzymatic activity of ceria, which would facilitate a safe and economical implementation for IBD treatment. Herein, we synthesized gold nanoparticles-embedded ceria nanoparticles (Au/CeO2) with enhanced SOD- and CAT-mimetic activities for treating IBD. The Au/CeO2 with core-shell and porous structure could offer a high surface-to-volume for exposure of catalytic sites, and promote cerium (III)/cerium (IV) redox reaction to enhance the antioxidant enzymatic activity of ceria [10]. After being coated with negatively-charged hyaluronic acid (HA), the Au/CeO2HA facilitated accumulation in the inflamed colon tissues via oral administration, reduced the production of pro-inflammatory cytokines, and effectively alleviated colon injury in the acute colitis mice. Notably, Au/CeO2HA exhibited good compatibility *in vitro* and *in vivo*, which showed negligible cytotoxicity and hemolytic activity and hardly affected the major organs. These together indicate that Au/CeO2HA is a promising nanoantioxidant for treating IBD [11].

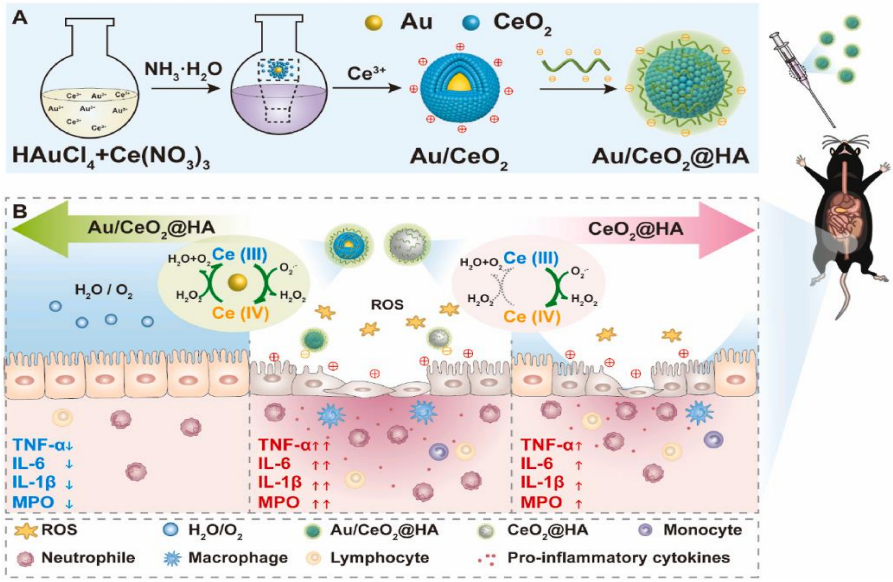

Fig. 1. Schematic illustration of the synthesis and therapy application of Au/CeO2HA nanozyme for mice with colitis. (A) Schematic illustration of synthesis progress of Au/CeO2HA. (B) Therapeutic effects of Au/CeO2HA or CeO2HA in colitis. The enhanced catalytic activity of Au/CeO2HA is attributed to the porous structure and accelerated the regeneration of Ce (III) from Ce (IV) induced by the Au core. The Au/CeO2HA sufficiently eliminates ROS and reduces pro-inflammatory cytokines to alleviate colon injury in colitis mice.

Journal of Chemical Health Risks

www.jchr.org

JCHR (2024) 14(4), 1516-1528 | ISSN:2251-6727

2. Materials and methods

Cerium nitrate hexahydrate and ammonia solution (AR, 25–28%) were purchased from Loba Chemie Pvt Ltd. (Mumbai, India). Gold chloride hydrate, cerium oxide (20–50 nm), dextran sulfate sodium (DSS), and rhodamine B were purchased from Sigma-Aldrich, (Delhi, India). Methylthiazolyldiphenyl-tetrazolium bromide (MTT) was obtained from Biosharp. 2′,7′-Dichlorofluorescin diacetate (DCFH-DA) was purchased from Sigma-Aldrich, (Delhi, India). Lysotracker was purchased from Sigma-Aldrich, (Delhi, India). The dopamine-grafted hyaluronic acid (40–100 kDa, modification degree: 37.6 μmol/g) was synthesized as our previous work. The ceria nanoparticles were synthesized as the previous studies (CeO2-1 and CeO2-2) [12].

Synthesis of Au/CeO2 and Au/CeO2HA

Au/CeO2 was synthesized according to the literature. HAuCl4 and Ce(NO3)3 were added to H2O (50 mL) in an ice bath. Next, ammonia solution (64 μL of 25–28% ammonia solution dissolved in 3 mL of H2O) was rapidly added and stirred for 25 s. Then Ce(NO3)3 solution (0.0467 M, 3000 μL) was added to the mixed solution and stirred for 15 min. The products were collected by centrifugation (10 ◦C, 10000 g, and 60 min) and washing with H2O for three times. To modify Au/CeO2 with hyaluronic acid (HA) shell, the Au/CeO2 (1 mg/mL, 20 mL) was slowly added into the dopamine grafted-HA solution (1 mg/mL, 20 mL) and then stirred for 12 h. Au/CeO2HA was collected by centrifuging (10 ◦C, 10000 g, and 60 min) and washing with H2O for three times. To obtain the rhodamine B labeled nanoparticles, Au/CeO2 suspension (1 mg/mL, 20 mL) was mixed with rhodamine B (1 mg/mL, 20 mL) and incubated for 4 h at room temperature. The rhodamine B-labeled Au/CeO2 was collected by centrifuging (10000 g, and 60 min) and washing with deionized water until the supernatant is transparent. To obtain rhodamine B-labeled Au/CeO2HA, rhodamine B- labeled Au/ CeO2 (1 mg/mL, 10 mL) was added into the dopamine-grafted HA solution (1 mg/mL, 10 mL) and then stirred for 12 h. The rhodamine Blabeled Au/CeO2HA was collected by centrifuging and washing.

Characterization

Hydrodynamic size and zeta potential were measured in the deionized water on Nano-ZS ZEN3600. The morphology of nanoparticles was characterized by the transmission electron microscope (Hitachi H-7000FA) and high-resolution transition electron microscope (HR-TEM). Jed2300 was used to observe the element distribution of Au/CeO2. X-ray powder diffraction (XRD) patterns were recorded by Bruker D8 Advance. X-ray photoelectron spectroscopy (XPS) spectra were performed by ESCALAB 250Xi (Thermo Fisher). Thermogravimetric analysis (TGA) was carried out by TA TGA55. Temperature-programmed reduction (TPR) analysis was measured by AutoChem1 II 2920. The N2 adsorption/desorption isotherm was performed by ASAP 2460 3.01 and the surface area and pore size were calculated using the Brunauer-Emmett-Teller (BET) model. Inductively coupled plasma mass spectrometry was employed to measure the retained concentrations of Au/CeO2 or Au/CeO2HA in the colon tissues. The cellular internalization of rhodamine B-labeled nanoparticles was evaluated using a Nikon Ti–U microscopy equipped with a CSU-X1 spinning-disk confocal unit and an EM-CCD camera.

The enzymatic catalytic activity

The antioxidant activities of Au/CeO2, CeO2, Au/CeO2HA, and CeO2HA were conducted according to the protocols of assays kit. The O2 •- scavenging activity was measured using a total superoxide dismutase (SOD) colorimetric assay kit. The H2O2 scavenging activity was measured using a catalase assay kit. The steady-state kinetic assay of Au/CeO2 was determined by varying the concentration of H2O2 (0–15 mM) in the presence of Au/CeO2 (50 μg/mL). After incubation at room temperature for 10 min, the residual H2O2 was quantified using a hydrogen peroxide assay kit. The *Km* was calculated using Lineweaver-Burk plots. To investigate the stability of Au/CeO2HA, Au/CeO2HA was dispersed and incubated in simulated gastric fluid (SGF) for 4 h or simulated intestinal fluid (SIF) for 72 h, and the hydrodynamic size, zeta potential, and enzymatic catalytic activity were measured [13].

Cell culture and cytotoxicity assay

Human immortalized colonic epithelial cells were cultured in the high glucose-DMEM media containing 10% fetal bovine serum under an atmosphere of 5% CO2 at 37 ◦C. NCM460 cells were cultured in 96-well plates (6 × 103 cells per well) for 24 h. After that, Au/CeO2 or Au/CeO2HA (25–400 μg/mL) was added and cultured

Journal of Chemical Health Risks

www.jchr.org

JCHR (2024) 14(4), 1516-1528 | ISSN:2251-6727

with cells for another 24 h. MTT assay was employed to quantify the cell viability.

Intracellular ROS scavenging ability

NCM460 cells were seeded at 2 × 105 cells per well in 6-well plates. After culture for 24 h, fresh media with nanoparticles (100 μg/mL) were added and cultured with cells for 12 h. Then 50 μg/mL of Rosup was

added to the cells followed by incubation for 30 min. Next, the NCM460 cells were incubated with 10 μM of 2′,7′-dichlorofluorescin diacetate for 30 min, and then washed with PBS. At last, intracellular DCF fluorescence was imaged using a fluorescence spectrophotometer. The untreated cells served as the control.

Cellular internalization behavior

HUVEC cells (human umbilical vein endothelial cells) or NCM460 cells (immortalized human colon mucosal epithelial cells) were seeded onto the cover-glass bottom dishes with a density of 6 × 104 cells and cultured for 24 h. Then the cells were incubated with rhodamine Blabeled Au/CeO2 or Au/CeO2HA (100 μg/mL) for 4 h. Next, the cells were washed with PBS and stained with lysotracker Green (75 nM) and Hoechst (5 μg/mL). Finally, the cells were rinsed with PBS and imaged by a confocal fluorescence microscope.

Cytoprotective effect of nanozyme

NCM460 cells (6 × 103 cells per well) were cultured in 96-well plates for 24 h. Then, the fresh media with different concentrations of nanozymes (0, 50, 75, 100, 200 μg/mL) and H2O2 (300 μM) were added to the

cells and incubated for another 24 h. MTT assay was employed to determine the cell viability.

Hemolysis assay

The hemolysis experiments were measured as the previous study. The nanoparticles (100 μL, in PBS) were mixed with mouse red blood cell suspension (2% in PBS, v/v, 900 μL). The final concentrations of Au/CeO2 or Au/CeO2HA in RBCs suspensions were 6.25–200 μg/mL. Then, the mixtures were shaken at 37 ◦C for 4 h and then centrifuged at 3000 rpm for 10 min. To determine the hemoglobin concentration of the supernatant, a microplate reader was used to measure the absorbance at 545 nm. Triton X-100 and PBS were chosen as the positive and negative controls [14].

Animal studies

Six-week-old male C57BL/6 mice were purchased from SPF Biotechnology Co., Ltd. All the animal experiments were performed following the guideline approved by the Institutional Animal Ethics Committee (IAEC) at Columbia Institute of Pharmacy, Tekari, Raipur, Chhattisgarh, India.

Biocompatibility of Au/CeO2HA in vivo

The C57BL/6 mice (6-week-old, 18–20 g) acclimatized for five days and were randomly divided into two groups, including the healthy control group and Au/CeO2HA group (n = 5). Control healthy mice were given water only, and Au/CeO2HA group mice received 2 mg/kg of Au/CeO2 via oral administration on day 2, 4, and 6, respectively. Changes in body weight were monitored daily. All mice were sacrificed on day 10. The colon, heart, liver, spleen, lung, and kidney were collected and fixed with 4% paraformaldehyde for hematoxylin and eosin (H&E) staining. The serum was collected for biochemical index detection.

Colon accumulation and excretion of Au/CeO2HA

The C57BL/6 mice (6-week-old, 18–20 g) were fed with DSS (40kDa)-containing water (3%, w/v) for six consecutive days to establish the colitis model. Next, the mice were randomly divided into two groups and were orally administered with Au/CeO2 or Au/CeO2HA (2 mg/kg). After different time points (6, 12, 24, 72, 168 h), mice were sacrificed and the whole colons were collected [15]. The colons were gently washed with PBS to remove retained feces. Next, the colon tissues were cut up into pieces and digested with aqua regia under 120 ◦C. After evaporation, the residues were dissolved in nitric acid (5%), and the Ce contents were determined by ICP-MS. The relative Ce accumulation was calculated by the following equation: Ce content (%) = Mt/M0, where Mt is the Ce mass in colons at the indicated time, and M0 is the total Ce mass of administered Au/CeO2HA or Au/CeO2. To visualize the distribution of Au/CeO2HA, the colitis mice were orally administered with rhodamine B-labeled Au/CeO2HA (2 mg/ kg), the GI tracts were isolated, and the fluorescent images of GI tracts were obtained by *in vivo* imaging system (IVIS, Bruker, Ex = 550 nm; Em = 600 nm).

DSS-induced model of colitis

Journal of Chemical Health Risks

www.jchr.org

JCHR (2024) 14(4), 1516-1528 | ISSN:2251-6727

The C57BL/6 mice (6-week-old, 18–20 g) were acclimatized for five days and randomly divided into four groups, including the healthy control group, DSS-induced colitis group, DSS-induced colitis mice treated with Au/CeO2HA, and DSS-induced colitis group treated with CeO2HA (*n* = 7). Colitis mice were induced by feeding with DSS containing water (3%) for 6 days, while the healthy mice were only fed with water. Then the colitis mice were orally treated with Au/ CeO2HA or CeO2HA (2 mg/kg) on predetermined days (day 7, day 9, and day 11). The body weights of mice were recorded daily over the experimental period. On day 12, the entire colons and serum were collected from the mice receiving treatments. The length of the colons was measured. The colon tissues were fixed with 4% paraformaldehyde for hematoxylin and eosin (H&E) staining or frozen for cytokines examination. To compare the therapeutic efficiency of Au/CeO2HA with 5-ASA, another animal experiment was performed. The colitis mice were induced as described above and were orally treated with Au/CeO2HA (2 mg/kg), CeO2HA (2 mg/kg), and 5-ASA (30 mg/kg) on predetermined time (day 7, day 9, and day 11). The body weights and disease activity index (DAI) of mice were recorded daily over the experimental period. The DAI was assigned scores as the literature. On day 12, the entire colons were collected from the mice receiving treatments for colon length measurement and H&E staining [16].

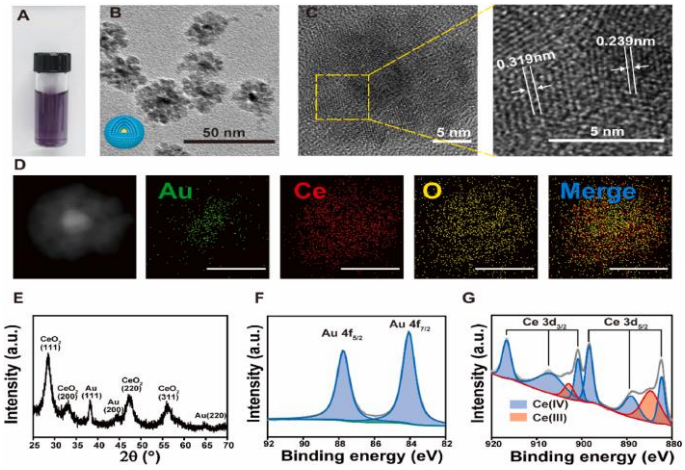

Fig. 2. Structure characterization of Au/CeO2. (A) A photograph of Au/CeO2 suspension. (B) TEM image of Au/CeO2. Inset: a schematic image of Au/CeO2. Scale bar, 50 nm. (C) HR-TEM image of Au/CeO2. Scale bar, 5 nm. (D) STEM-EDX elemental maps of Au/CeO2. Green for Au, red for Ce, and yellow for O. Scale bar, 20 nm. (E) XRD pattern of Au/CeO2. (F) Au 4f XPS spectra of Au/CeO2. (G) Ce 3d XPS spectra of Au/CeO2.

Myeloperoxidase (MPO) activity measurement and enzyme linked immunosorbent assay (ELISA) analysis

To evaluate the inflammation level in mice, MPO activity and proinflammatory cytokines of the colon tissue isolated from the colitis mice receiving treatments were measured. The middle colon of each mouse was homogenized in RIPA lysis buffer (4 ◦C). Then, the resultant homogenate was centrifuged at 12000 rpm for 20 min at 4 ◦C, and the supernatant was collected for further detection. BCA assay was used to determine the protein concentration of the supernatant samples. The MPO activity of colon tissues was measured as previously reported [17]. The supernatant (50 μL) was added to PBS (150 μL, pH 6.0, 50 mM) containing 0.2 mg/mL of *o*-dianisidine dihydrochloride and 0.005% H2O2 and incubated for 1 h. Next, the absorbance at 460 nm was recorded. The relative MPO activity was calculated by the following equation: relative MPO activity = A460/C, where A460 is the absorbance at 460 nm of each sample, and C is the protein concentration of the supernatant samples. Were used to quantify the amounts of IL-6, TNF-α, and IL-1β in the homogenate of colon tissues and serum according to the manufacturer's instructions. Briefly, the supernatant or serum (50 μL) was added into the wells that were pre-coated with the antibody of indicated proinflammatory cytokines and incubated for 2 h at room temperature. The residual sample was removed by the washing buffer. The detection antibody solution (100 μL) was added into the wells and incubated for 1 h at room temperature. After washing for 4 times, avidin-HRP solution (100 μL) was

Journal of Chemical Health Risks

www.jchr.org

JCHR (2024) 14(4), 1516-1528 | ISSN:2251-6727

added into the wells and incubated for 30 min. Next, the plate was washed 5 times with washing buffer. Subsequently, substrate (100 µL) was added into the wells and incubated for 15 min in dark. Finally, the stop solution (100 µL) was mixed with the above substrates, and the absorbance at 450 nm was recorded. The concentrations of proinflammatory cytokines in colon tissues and serum were shown as pg/ mg protein and pg/mL, respectively [18].

Statistical analysis

The significant difference was determined by the student's t-test.

Statistically significant differences were defined as follows: *p < 0.05, **p < 0.01, ***p < 0.001, ns, not significant.

3. Result and discussion

Synthesis and characterization of Au/CeO2

The Au/CeO2 was synthesized through an auto-redox reaction between AuCl4 - and Ce3+ in the presence of ammonium hydroxide. The synthesized Au/CeO2 could be well dispersed in the aqueous solution with a characteristic absorption peak at 545 nm. The transmission electron microscopy (TEM) images indicated that Au/CeO2 displayed a core-shell nanostructure (22 nm, PDI: 0.03), and the Au core could be obviously observed in 92% of nanoparticles [19]. High-resolution TEM (HR-TEM) images further fluorescence intensity of NCM460 cells under Rosup-treatment. Blue: Hoechst, and green: DCF (n = 9). Scale bar, 100 µm. (I–J) Relative Ce contents in the colonic tissues of mice after treating with Au/CeO2 (I) or Au/CeO2HA (J) orally. Data represent mean ± SEM. revealed the lattice distance of shell corresponding to the (111) planes of CeO2 (0.319 nm) and the lattice distance of core corresponding to the (111) planes of Au (0.239 nm). Moreover, the energy-dispersive X-ray spectroscopy (EDX) element mappings confirmed that the Au elements were mainly distributed in the core of nanoparticles, while the Ce and O elements exhibited uniform distributions [20]. The crystalline feature of Au/CeO2 was characterized by an X-ray powder diffraction (XRD) pattern, indicating the characteristic peaks of CeO2 (JCPDS No.34-0394) and Au (JCPDS No.04-0784). To further examine the composition and valence states, X-ray photoelectron spectroscopy (XPS) was employed to characterize the Au/CeO2. The two peaks in Au 4f spectrum were consistent with Au (0) and the Ce 3d spectrum revealed the co-existence of Ce (III) and Ce (IV) oxidation states in ceria. All these results indicate that Au/CeO2 nanoparticles are successfully synthesized, and the CeO2 is formed on the outer shell while the Au NP is encapsulated in the core [21].

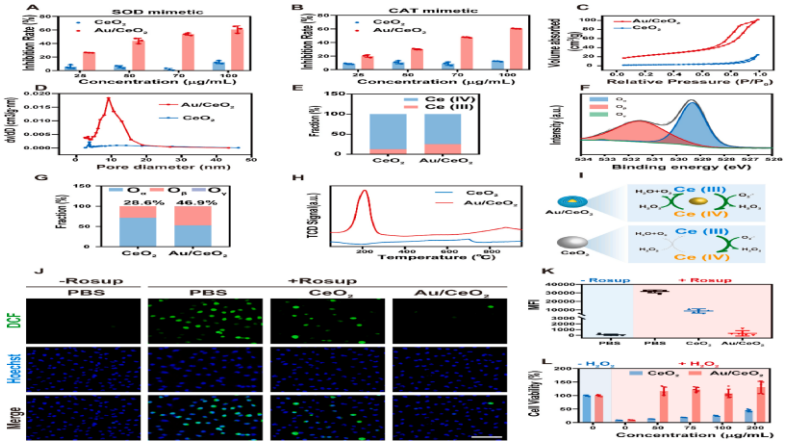

Fig. 3. ROS scavenging performance of Au/CeO2 *in vitro*. (A) SOD-mimetic activities of Au/CeO2 and CeO2 (n = 3). (B) CAT-mimetic activities of Au/CeO2 and CeO2 (n = 3). (C) N2 adsorption isotherms of Au/CeO2 and CeO2. (D) Pore size distributions of Au/CeO2 and CeO2. (E) Ce (III) and Ce (IV) fractions of Au/CeO2 and CeO2. (F) O 1s XPS spectrum of Au/CeO2. (G) Oβ fractions of Au/CeO2 and CeO2. (H) Temperature-programmed reduction of H2 curves. (I) Schematic illustration of enhanced catalytic activity of Au/CeO2. (J) Representative ROS staining and relative mean fluorescence intensity (K) of NCM460 cells in the presence of Rosup and Au/CeO2 or CeO2. Scale bar, 100 µm. (L) Viabilities of NCM460 cells in the presence of H2O2 and Au/CeO2 (n = 5). Data represent mean ± SD.

Journal of Chemical Health Risks

www.jchr.org

JCHR (2024) 14(4), 1516-1528 | ISSN:2251-6727

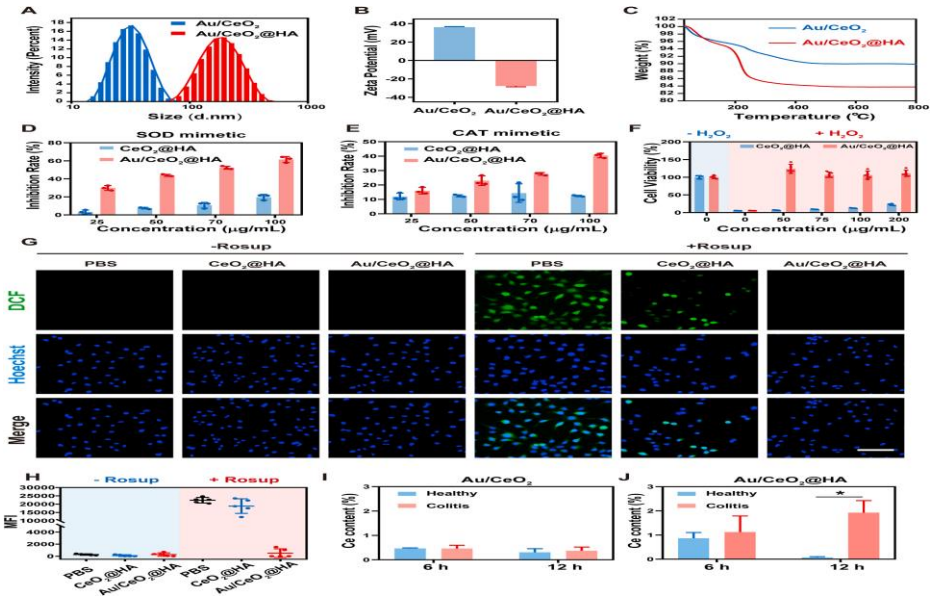

Fig. 4. Modification Au/CeO2 with HA. (A) DLS size distribution of Au/CeO2 and Au/CeO2HA. (B) Zeta potentials of Au/CeO2 and Au/CeO2HA. (C) TGA curves of Au/CeO2 and Au/CeO2HA. (D) SOD mimics activities of Au/CeO2HA and CeO2HA (*n* = 3). (E) CAT mimics activities of Au/CeO2HA and CeO2HA (*n* = 3). (F) Relative viability of NCM460 cells under H2O2-treatment in the presence of Au/CeO2HA (*n* = 5). (G) Representative ROS staining and (H) relative mean.

Enhanced antioxidant enzymatic activity of Au/CeO2

The ROS eliminating capacity of Au/CeO2 was investigated towards superoxide anions (O2 •-) and hydrogen peroxide (H2O2), and the commercial CeO2 was chosen as a control. The SOD-like catalytic activity (O2 •- scavenging) of these nanozymes was studied using the watersoluble tetrazolium 1 (WST-1) method. The Au/CeO2 efficiently eliminated the O2 •- in a dose-dependent manner, and scavenged over 60% of O2 •- at the concentration of 100 μg/mL within 20 min. In sharp contrast, the commercial CeO2 exhibited limited efficiency on O2 •- clearance at all the tested concentrations (25–100 μg/mL). Next, the CAT-like catalytic activity was investigated by determining H2O2 scavenging. Similarly, Au/CeO2 exhibited dramatically higher H2O2 eliminating efficacy compared with commercial CeO2. Furthermore, kinetics analysis was performed and the results fitted the Michaelis- Menten kinetics. The Michaelis-Menten constant (*Km*) value and CAT-like activity of Au/CeO2 were calculated to be 3.224 mM and 6.330 U/mg, respectively. These results indicate that Au/CeO2 possesses multi-enzymatic activities for eliminating both O2 •- and H2O2, which are markedly higher than that of its commercial counterpart. Moreover, we synthesized two types of CeO2 nanoparticles as the previous studies [22], and found that Au/CeO2 also exhibited higher ROS scavenging efficacy compared with these ceria nanoparticles confirming the good antioxidant activity of Au/CeO2. The catalytic efficacy is highly dependent on the exposed active sites of nanozymes. Thus, nitrogen adsorption isotherms analysis was performed to investigate the surface-to-volume ratio. The BrunauerEmmett-Teller (BET) surface area of Au/CeO2 was about 10-fold higher than that of CeO2 and the mesopores (5–20 nm) could be detected in Au/CeO2 which formed by the stacking of CeO2 around Au core [23]. The high surface-to-volume and large void in the core-shell structure of Au/CeO2 would sufficiently expose the catalytic sites to facilitate interactions between ROS and nanozymes. Moreover, the valence ratio of Ce (III)/Ce (IV) and oxygen species also plays essential roles in the catalytic activity of ceria nanoparticles. Both Au/CeO2 and commercial CeO2 possessed dual oxidation states of Ce but the ratio of Ce (III)/Ce (IV) in Au/CeO2 (25.1/74.9) was twice as high as that in CeO2 (12.7/87.3). The O1s spectra revealed the characteristic peaks of lattice oxygen (Oα), surface oxygen species (Oβ), and chemisorbed water and/or carbonated (Oγ). Among them, Oβ from defective sites was reported to play a significant role in most catalytic

Journal of Chemical Health Risks

www.jchr.org

JCHR (2024) 14(4), 1516-1528 | ISSN:2251-6727

progress [24]. Quantitative analysis suggests that the increased Ce (III) promotes Oβ percentage in Au/CeO2 (46.9%) compared to CeO2 (28.6%). The rate of reduction from Ce (IV) to Ce (III) was also a crucial challenge for the regeneration of enzyme-mimic activity of ceria nanoparticles. Thus, the temperature-programmed reduction (TPR) analysis was performed. In the H2-TPR spectrum of Au/CeO2, a reduction peak was observed at 210 ◦C, which was significantly lower than the reported reduction temperature of ceria nanoparticles (398 ◦C) while no significant reduction peak appeared in the spectrum of commercial CeO2. The decreased reduction temperature might be induced by the accelerated electron transfer by the Au nanocore in Au/CeO2 and the great reducing capability of Au–H species on the surface of Au nanocore [25]. These results suggest that Au/CeO2 not only possesses higher contents of Ce (III) and oxygen vacancy but also accelerates the reduction from Ce (IV) to Ce (III) compared with commercial CeO2, thus resulting in enhanced catalytic activities of Au/CeO2. Encouraged by the excellent antioxidant activity, NCM460 cells were employed to assess the cellular ROS eliminating capability of Au/CeO2. In the presence of Rosup, a ROS-generated reagent, the intracellular ROS was significantly elevated in NCM460 cells with obviously green fluorescence indicated by 2′, 7’ –dichlorofluorescein (DCF). The Au/CeO2 entered into the cells and mainly localized in the lysosomes and sufficiently eliminated the overproduced ROS by 99.2% in Rosup-treated cells, of which the intracellular ROS level was as low as the untreated cells while CeO2 only scavenged 72.8% of ROS. Due to the excellent ROS elimination efficacy, Au/CeO2 almost abrogated the damage induced by oxidative stress and recovered the cell viability of H2O2-treated cells. In contrast, CeO2 only elevated the cell viability to 44% at the high concentration of 200 μg/mL, likely because of its limited antioxidant activity. Taken together, these results indicate that the Au/CeO2 with excellent enzymatic activities could sufficiently scavenge ROS to protect cells from oxidative stress [26].

HA modification on Au/CeO2 enhances specific accumulation in inflamed colons

The depletion and discontinuity of mucus layer accumulation of positively charged proteins (including transferrin bacteriostatic and eosinophil cationic protein at inflammatory sites, and overexpressed CD44 on inflamed epithelial cells are the prominent features of colitis. Hyaluronic acid (HA), an anionic natural polysaccharide with a specific affinity of CD44, would be an ideal target group for inflammatory intestinal through electrostatic and HA-CD44 interactions [27]. To promote the specific accumulation of Au/CeO2 toward the inflammation site, dopamine-grafted HA was employed to modify the positively-charged Au/CeO2 via electrostatic interaction. After HA modification on Au/CeO2, the hydrodynamic diameter of nanoparticles increased from 30.4 nm to 160 nm likely due to forming clusters and the zeta-potential reversed from positive (+36.1 mV) to negative (- 27.7 mV) while the UV–Vis spectrum was hardly changed by HA coating. Moreover, the weight loss of HA-coated nanoparticles increased by 6.3% in thermogravimetric analysis (TGA) compared to Au/CeO2. These results revealed that Au/CeO2 was successfully modified with HA. As a control, the CeO2 was also modified with HA of note, the HA modification on Au/CeO2 had a negligible influence on the SOD mimetic activity and slightly reduced the CAT-like activity which was much higher than that of CeO2HA. Hence, Au/CeO2HA sufficiently eliminated the intracellular ROS and protected cells from H2O2-induced damages, while CeO2HA hardly weakened the oxidative stress *in vitro*. These results indicate that HA modification maintained the excellent ROS-scavenging activity and cytoprotection ability of Au/ CeO2. Importantly, the relative catalytic activity of Au/CeO2HA remained higher than 85% after incubation with simulated gastric fluid (SGF) for 4 h or simulated intestinal fluid (SIF) for 72 h, and the hydrodynamic size and zeta potential were just decreased slightly after treatments suggesting the good stability of Au/CeO2HA. Next, we suspected the HA coating on Au/CeO2 would facilitate the retention in inflamed colon tissues due to the HA-CD44 mediated interaction and the electrostatic interaction [28]. To test this notion, the healthy and acute colitis (induced by dextran sulfate sodium (DSS) mice were treated with Au/CeO2 and Au/CeO2HA (by oral, 2 mg/kg), respectively. Six or 12 h after treatment, the colon tissues were isolated for testing nanoparticle accumulation by determining the Ce contents using ICP-MS. Six hours after treatment, Au/CeO2HA was detected in both healthy colons and colitis colons. For the positively-charged Au/ CeO2, the Ce accumulation exhibited no significant difference in health and colitis colons. On the contrary, Au/CeO2HA effectively accumulated in the inflamed colon tissues at 12 h post-treatment, which was almost eliminated from the healthy

Journal of Chemical Health Risks

www.jchr.org

JCHR (2024) 14(4), 1516-1528 | ISSN:2251-6727

colons at this time. Notably, the Ce content in the colons of colitis mice receiving Au/ CeO2HA was significantly higher (5.2-fold) than that of colitis mice receiving Au/CeO2. These Au/CeO2HA nanoparticles could be gradually excreted and almost eliminated from the colons in colitis mice after 72 h which would not induce long term accumulation. These results indicate that the HA coating specifically enhances ceria nanozyme accumulation in inflamed colon tissues and maintained catalytic activities [29].

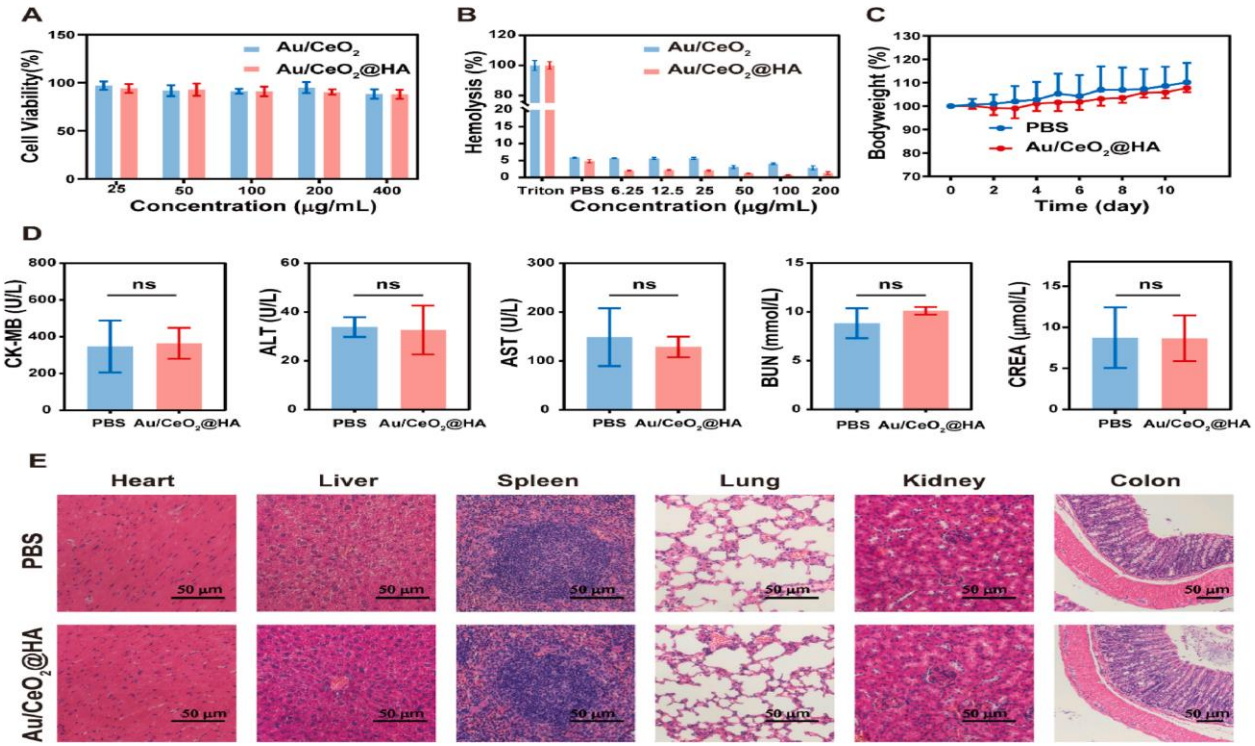

Fig. 5. Biosafety of Au/CeO2HA. (A) Cell viabilities of NCM460 cells after incubation with Au/CeO2 or Au/CeO2HA (*n* = 5). (B) Hemolysis activity of Au/CeO2 and Au/CeO2HA. (*n* = 3) (C) Relative body weights of healthy mice receiving Au/CeO2HA treatment (2 mg/kg, oral administration, three times) (*n* = 5). (D) Analysis of main biochemical indexes in serum (*n* = 5). (E) Hematoxylin-eosin (H&E) staining of the major organs from mice receiving Au/CeO2HA treatment. Scale bars, 50 μm.

Biocompatibility of Au/CeO2HA

Biocompatibility is a prerequisite for nanomedicine. Thus, the potential toxicity of Au/CeO2HA was investigated before therapeutic study *in vivo*. To test *in vitro* biocompatibility, the cytotoxicity and hemolysis activity were studied. The viability of NCM460 cells exposed to Au/CeO2HA was higher than 88% even at the concentration up to 400 μg/mL and no obvious hemolysis was observed at all the test concentrations. Of note, the hemolysis rate slightly decreased by HA-coating likely due to the surface charge reversal of nanoparticles. Next, the healthy C57BL/6 mice were treated with Au/ CeO2HA via oral administration (3 times, 2 mg/kg). The body weights of mice were not affected by Au/CeO2HA treatment as well as healthy mice. Moreover, the main biochemical indicators of serum reflecting the functions of the heart, liver and kidney were not markedly changed by Au/CeO2HA treatment suggesting that Au/CeO2HA does not affect the functions of major organs. Consistently, no significant difference was observed in the hematoxylin-eosin staining images of the organs (heart, liver, spleen, lung, kidney, and colon) between Au/CeO2HA group and untreated mice. These results illustrated that Au/ CeO2HA treatment did not damage the major organs and affect their functions, suggesting the good biocompatibility of Au/CeO2HA *in-vivo* [30].

Journal of Chemical Health Risks

www.jchr.org

JCHR (2024) 14(4), 1516-1528 | ISSN:2251-6727

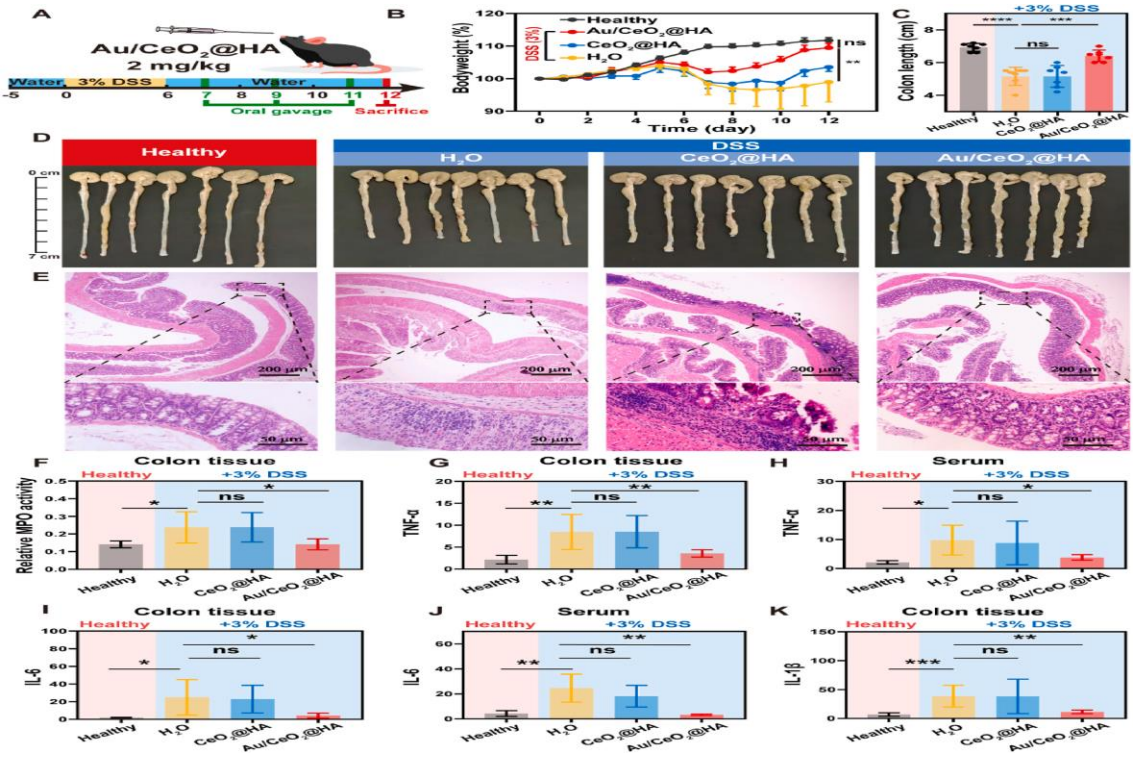

Fig. 6. Therapeutic effect of Au/CeO2HA in ulcerative colitis. (A) Overall protocol of the animal experiment. C57BL/6 mice received water or 3% DSS-containing water for 6 consecutive days. On the day 7, 9, and 11, mice were orally administered with Au/CeO2HA or CeO2HA (2 mg/kg) (n = 7). (B) Relative body weights of mice receiving treatments. (C) Colon lengths and (D) photos of colon tissues with indicated treatments on day 12. (E) Hematoxylin-eosin (H&E) staining images of colon tissues. (F) Relative myeloperoxidase (MPO) activity in colon homogenates. TNF-α levels in colon homogenates (G) and serum (H) of each group. IL-6 levels in colon homogenates (I, pg/mg protein) and serum (J, pg/mL) of each group. (K) IL-1β levels in colon homogenates of each group. Data represent mean ± SD (*$p < 0.05$, **$p < 0.01$, and ***$p < 0.001$).

Therapeutic effects of Au/CeO2HA in DSS-induced acute colitis

Based on the excellent ROS-scavenging ability and biocompatibility, the therapeutic effect of Au/CeO2HA was tested in the acute ulcerative colitis model induced by DSS. The body weights of colitis mice receiving DSS for 6 days decreased significantly indicating the successful establishment of the colitis model. In contrast to colitis mice receiving water with irrevocably decreased body weights, Au/ CeO2HA promptly stopped the weight loss on day 8 and recovered the body weights of colitis mice to the level of healthy mice on day 12. Moreover, Au/CeO2HA treatment sufficiently abrogated the shortening of colon length which is a characteristic feature of colon injury induced by muscle wasting associated with inflammation progression. However, CeO2HA was completely ineffective to alleviate the weight loss and colon shortening. Similar to the colons of colitis mice showing severe disorder of intestinal structure, including crypt disappearance, significantly loose goblet cells, and inflammatory cell infiltration the colitis mice treated with CeO2HA still suffered from crypt atrophy and inflammatory cell infiltration. In stark contrast, the colon structure of mice receiving Au/CeO2HA was preserved as well as the healthy mice [31]. Moreover, the therapeutic effect of Au/CeO2HA was confirmed by comparing it with 5-amino salicylic acid (5-ASA), a clinically used therapeutic agent for colitis. Consistently, Au/CeO2HA sufficiently alleviated the colon damage and recovered the body weight and colon length of colitis mice, while 5-ASA exhibited limited therapeutic efficacy likely due to its poor availability. To further investigate the therapeutic effect of Au/CeO2HA, myeloperoxidase (MPO) and typical pro-inflammatory cytokines were measured. MPO is a unique granule heme enzyme of neutrophils and

Journal of Chemical Health Risks

www.jchr.org

JCHR (2024) 14(4), 1516-1528 | ISSN:2251-6727

monocytes, which can produce powerful ROS, especially hypochlorous acid (HOCl). The upregulated HOCl not only induces cell apoptosis, but also exacerbates the inflammatory response. Compared with healthy colon tissues, DSS feeding dramatically elevated the MPO activity. Such enhanced MPO activity induced by DSS was effectively downregulated by Au/CeO2HA to the level as low as that of healthy colons. Similarly, the pro-inflammatory cytokines (IL-1β, IL-6, and TNF-α) in colon tissue and serum were also increased by DSS, which were normalized by Au/CeO2HA treatment. Taken together, these results demonstrate that the Au/CeO2HA could effectively alleviate DSS-induced colitis by reducing infiltration of inflammatory cells and pro-inflammatory cytokines production [32].

4. Conclusion

In summary, we developed a gold nanoparticle-embedded ceria nanozyme (Au/CeO2) with ROS-scavenging activities for treating ulcerative colitis. The Au/CeO2 exhibited significantly enhanced enzymatic catalytic activities (SOD and CAT) compared with the commercial ceria, likely due to the porous structure and fast reduction rate from cerium (IV) to cerium (III) induced by the gold core. After being coated with hyaluronic acid (HA), the negatively-charged Au/CeO2HA could sufficiently accumulate in the inflamed colon tissues and inherit excellent catalytic activities for eliminating ROS (O2 •- and H2O2). In the DSSinduced colitis, Au/CeO2HA effectively recovered the body weight and colon length of colitis mice by reducing the infiltration of inflammatory cells and the production of proinflammatory cytokines, while the HA-coated commercial ceria (CeO2HA) hardly alleviated the colitis. Thus, this work not only demonstrated a versatile method to facilitate the catalytic activity of ceria but also provided an excellent antioxidant nanotherapeutic for treating colitis.

Declaration of competing interest

The author declares no conflict of interest, financial or otherwise.

Acknowledgements

This research did not receive any specific grant from funding agencies in the public, commercial, or not-for profit sectors. The authors are helpful to the National Institute of Technology (NIT), Rourkela, Odisha, India for providing all required facilities.

References

[1] C.N. Bernstein, M. Fried, J.H. Krabshuis, H. Cohen, R. Eliakim, S. Fedail, R. Gearry, K.L. Goh, S. Hamid, A.G. Khan, A.W. LeMair, Malfertheiner, Q. Ouyang, J.F. Rey, A. Sood, F. Steinwurz, O.O. Thomsen, A. Thomson, G. Watermeyer, World gastroenterology organization practice guidelines for the diagnosis and management of IBD in 2010, Inflamm. Bowel Dis. 16 (1) (2010) 112–124.

[2] M.L. Hoivik, B. Moum, I.C. Solberg, M. Henriksen, M. Cvancarova, T. Bernklev, I. Group, Work disability in inflammatory bowel disease patients 10 years after disease onset: results from the IBSEN Study, Gut 62 (3) (2013) 368–375.

[3] D.C. Baumgart, W.J. Sandborn, Inflammatory bowel disease: clinical aspects and established and evolving therapies, Lancet 369 (9573) (2007) 1641–1657.

[4] C.M. Olesen, M. Coskun, L. Peyrin-Biroulet, O.H. Nielsen, Mechanisms behind efficacy of tumor necrosis factor inhibitors in inflammatory bowel diseases, Pharmacol. Ther. 159 (2016) 110–119.

[5] A. Stallmach, S. Hagel, T. Bruns, Adverse effects of biologics used for treating IBD, Best Pract. Res. Clin. Gastroenterol. 24 (2) (2010) 167–182.

[6] R.P. Hirten, M. Iacucci, S. Shah, S. Ghosh, J.F. Colombel, Combining biologics in inflammatory bowel disease and other immune mediated inflammatory disorders, Clin. Gastroenterol. Hepatol. 16 (9) (2018) 1374–1384.

[7] S.P. Colgan, C.T. Taylor, Hypoxia: an alarm signal during intestinal inflammation, Nat. Rev. Gastroenterol. Hepatol. 7 (5) (2010) 281–287.

[8] M. Iborra, I. Moret, F. Rausell, G. Bastida, M. Aguas, E. Cerrillo, P. Nos, B. Beltran, Role of oxidative stress and antioxidant enzymes in Crohn's disease, Biochem. Soc. Trans. 39 (4) (2011) 1102–1106.

[9] M.A. Alzoghaibi, Concepts of oxidative stress and antioxidant defense in Crohn's disease, World J. Gastroenterol. 19 (39) (2013) 6540–6547.

[10] Y. Naito, T. Takagi, T. Yoshikawa, Molecular fingerprints of neutrophil-dependent oxidative stress in inflammatory bowel disease, J. Gastroenterol. 42 (10) (2007) 787–798.

Journal of Chemical Health Risks

www.jchr.org

JCHR (2024) 14(4), 1516-1528 | ISSN:2251-6727

[11] A. Roessner, D. Kuester, P. Malfertheiner, R. Schneider-Stock, Oxidative stress in ulcerative colitis-associated carcinogenesis, Pathol. Res. Pract. 204 (7) (2008) 511–524.

[12] A. Rezaie, R.D. Parker, M. Abdollahi, Oxidative stress and pathogenesis of inflammatory bowel disease: an epiphenomenon or the cause? Dig. Dis. Sci. 52 (9) (2007) 2015–2021.

[13] I.E. Koutroubakis, N. Malliaraki, P.D. Dimoulios, K. Karmiris, E. Castanas, E.A. J. Kouroumalis, Decreased total and corrected antioxidant capacity in patients with inflammatory bowel disease, Dig. Dis. Sci. 49 (9) (2004) 1433–1437.

[14] A. Bhattacharyya, R. Chattopadhyay, S. Mitra, S.E. Crowe, Oxidative stress: an essential factor in the pathogenesis of gastrointestinal mucosal diseases, Physiol. Rev. 94 (2) (2014) 329–354.

[15] T.T. Jubeh, M. Nadler-Milbauer, Y. Barenholz, A. Rubinstein, Local treatment of experimental colitis in the rat by negatively charged liposomes of catalase, TMN and SOD, J. Drug Target. 14 (3) (2006) 155–163.

[16] K.E. Barrett, D.F. McCole, Hydrogen peroxide scavenger, catalase, alleviates ion transport dysfunction in murine colitis, Clin. Exp. Pharmacol. Physiol. 43 (11) (2016) 1097–1106.

[17] Y. Suzuki, T. Matsumoto, S. Okamoto, T. Hibi, A lecithinized superoxide dismutase (PC-SOD) improves ulcerative colitis, Colorectal Dis. 10 (9) (2008) 931–934.

[18] Y. Lin, J. Ren, X. Qu, Catalytically active nanomaterials: a promising candidate for artificial enzymes, Acc. Chem. Res. 47 (4) (2014) 1097–1105.

[19] Z. Jiulong, G. Wei, C. Xiaojun, X. Jiajia, Z. Duowu, L. Zhaoshen, H. Bing, Z. Yuanyi, Nanozyme-mediated catalytic nanotherapy for inflammatory bowel disease, Theranostics 9 (10) (2019) 2843–2855.

[20] C. Yuan, C. Chaoqun, Y. Jia, Y. Yijun, L. Yufeng, Z. He, M. Leiying, W. Hui, Mn3O4 nanozyme for inflammatory bowel disease therapy, Adv. Ther. 4 (9) (2021), 2100081.

[21] H.J. Kwon, M.Y. Cha, D. Kim, D.K. Kim, M. Soh, K. Shin, T. Hyeon, I. Mook-Jung, Mitochondria-targeting ceria nanoparticles as antioxidants for alzheimer's disease, ACS Nano 10 (2) (2016) 2860–2870.

[22] Q. Bao, P. Hu, Y. Xu, T. Cheng, C. Wei, L. Pan, J. Shi, Simultaneous blood-brain barrier crossing and protection for stroke treatment based on edaravone-loaded ceria nanoparticles, ACS Nano 12 (7) (2018) 6794–6805.

[23] E. Casals, M. Zeng, M. Parra-Robert, G. Fernandez-Varo, M. Morales-Ruiz, W. Jimenez, V. Puntes, G. Casals, Cerium oxide nanoparticles: advances in biodistribution, toxicity, and preclinical exploration, Small 16 (20) (2020), 1907322.

[24] I. Celardo, M. De Nicola, C. Mandoli, J.Z. Pedersen, E. Traversa, L. Ghibelli, Ce3+ ions determine redox-dependent anti-apoptotic effect of cerium oxide nanoparticles, ACS Nano 5 (6) (2011) 4537–4549.

[25] E.G. Heckert, A.S. Karakoti, S. Seal, W.T. Self, The role of cerium redox state in the SOD mimetic activity of nanoceria, Biomaterials 29 (18) (2008) 2705–2709.

[26] A. Migani, G.N. Vayssilov, S.T. Bromley, F. Illas, K.M. Neyman, Greatly facilitated oxygen vacancy formation in ceria nanocrystallites, Chem. Commun. 46 (32) (2010) 5936–5938.

[27] T. Ohkusa, Production of experimental ulcerative colitis in hamsters by dextran sulfate sodium and changes in intestinal microflora, Nihon Shokakibyo Gakkai Zasshi 82 (5) (1985) 1327–1336.

[28] Y. Lee, K. Sugihara, M.G. Gillilland 3rd, S. Jon, N. Kamada, J.J. Moon, Hyaluronic acid-bilirubin nanomedicine for targeted modulation of dysregulated intestinal barrier, microbiome and immune responses in colitis, Nat. Mater. 19 (1) (2020) 118–126.

[29] W. Guo, M. Zhang, Z. Lou, M. Zhou, P. Wang, H. Wei, Engineering nanoceria for enhanced peroxidase mimics: a solid solution strategy, ChemCatChem 11 (2) (2019) 737–743.

[30] Y. Zhang, K. Zhou, Y. Zhai, F. Qin, L. Pan, X. Yao, Crystal plane effects of nanoCeO2 on its

Journal of Chemical Health Risks

www.jchr.org

JCHR (2024) 14(4), 1516-1528 | ISSN:2251-6727

antioxidant activity, RSC Adv. 4 (92) (2014) 50325–50330.

[31] H. Zhu, X. Ke, X. Yang, S. Sarina, H. Liu, Reduction of nitroaromatic compounds on supported gold nanoparticles by visible and ultraviolet light, Angew. Chem., Int. Ed. 49 (50) (2010) 9657–9661.

[32] B. Tirosh, N. Khatib, Y. Barenholz, A. Nissan, A. Rubinstein, Transferrin as a luminal target for negatively charged liposomes in the inflamed colonic mucosa, Mol. Pharm. 6 (4) (2009) 1083–1091.